Progress in Organic Coatings 183 (2023) 107807

Contents lists available at ScienceDirect

Progress in Organic Coatings

journal homepage: www.elsevier.com/locate/porgcoat

A facile strategy for fine-tuning the drug release efficacy of poly-L-lactic acid-polycaprolactone coatings by liquid flame spray

Yonghong Pan [a,b], Daofeng Zhou [a,b,c], Tingting Cui [a,b,c], Yu Zhang [a,b,c], Lei Ye [a,b], Ye Tian [a,b], Ping Zhou [a,b], Yi Liu [a,b], Hidetoshi Saitoh [b,d], Botao Zhang [a,b,*], Hua Li [a,b,*]

[a] Zhejiang Engineering Research Center for Biomedical Materials, Cixi Institute of Biomedical Engineering, Ningbo Institute of Materials Technology and Engineering, Chinese Academy of Sciences, Ningbo 315201, China
[b] Zhejiang-Japan Joint Laboratory for Antibacterial and Antifouling Technology, Cixi Institute of Biomedical Engineering, Ningbo Institute of Materials Technology and Engineering, Chinese Academy of Sciences, Ningbo 315201, China
[c] Cixi Biomedical Research Institute, Wenzhou Medical University, Wenzhou 325035, China
[d] Department of Materials Science and Technology, Graduate School of Engineering, Nagaoka University of Technology, 1603-1 Kamitomioka-machi, Nagaoka, Niigata 940-2188, Japan

ARTICLE INFO

Keywords:
Poly (L-lactic acid) (PLLA)
Polycaprolactone (PCL)
Chloramphenicol (CAM)
Flame spray deposition
Controllable drug release
Bactericidal activity

ABSTRACT

The diversity of medical application scenarios demands fine-tuning of drug release profiles for better patient care. Here we report a facile strategy to construct composite coatings as universal drug delivery systems with tunable release efficacy. A poly-L-lactic acid (PLLA)-polycaprolactone (PCL) coating was fabricated by liquid flame spray and its performance was verified by loading chloramphenicol (CAM) as bactericidal component. Physiochemical analyses revealed the homogeneity of chemistry and integrity of functional groups of the composite coatings. Release of CAM was enhanced by the increase of the PCL content in the composite coatings, showing a controllable manner. Kinetics analysis suggested the release mechanism of Korsmeyer-Peppas model for both the PLLA-CAM and the PCL-CAM coatings, and the release regime for the PLLA-PCL composite coatings transited from the Higuchi model to the Korsmeyer-Peppas model when the PCL content increased from 30 % to 70 %. Further antibacterial testing revealed tailorable antibacterial activity of the coatings against both *Escherichia coli* and *Staphylococcus aureus*. Regulating the release of the drug CAM through altering PCL content in the PLLA-PCL coating would give inspiring insight into green fabrication of polymeric coatings with tunable drug release for versatile applications.

1. Introduction

Controllable drug release offers the possibility of enabling the active drug to achieve a desired therapeutic response for preventing or treating diseases, including the location, rate, and duration of release of a particular drug in the body [1,2]. The strategy of colonic, cancer and transplantation delivery require the rapid release of the drug to a target in a short period of time, maximizing the release rate and efficiency of the active ingredient [3,4]. On the contrary, one strategy for treating implant-associated infections, wounds and inflammation is the sustained and prolonged release of low-concentration drugs to obtain therapeutic efficacy [5,6]. To address the diverse requirement of clinical drug delivery, many different carriers and drug delivery systems have been investigated [7–9]. However, the variety of delivery routes and manufacturing processes will undoubtedly increase the complexity of clinical application and hinder the development of precision therapy based on individualized needs.

To accomplish controlled drug release, searching for carriers whose drug release can be facilely programmed has the potential to address a variety of unmet clinical needs and is one of the most tricky challenges for the drug delivery applications [10]. Compared with the existing delivery materials like liposomes [7], nanocrystals [8], and metal-organic frameworks [9], biopolymer-based biodegradable materials opt to be more promising for the drug delivery [11,12]. Among them, biodegradable poly (L-lactic acid) (PLLA) and polycaprolactone (PCL) can be extracted from renewable resources such as corn, cassava and

* Corresponding authors at: Zhejiang Engineering Research Center for Biomedical Materials, Cixi Institute of Biomedical Engineering, Ningbo Institute of Materials Technology and Engineering, Chinese Academy of Sciences, Ningbo 315201, China.
E-mail addresses: zhangbotao@nimte.ac.cn (B. Zhang), lihua@nimte.ac.cn (H. Li).

https://doi.org/10.1016/j.porgcoat.2023.107807
Received 3 March 2023; Received in revised form 4 July 2023; Accepted 9 July 2023

sugarcane. They are environment-friendly and possess excellent properties such as high mechanical strength, desired biodegradability and biocompatibility, low toxicity, fast bone regeneration, and ease for printing [13–15]. Owing to the abovementioned properties, they have been widely used in biomedical devices, such as surgical sutures, artificial skin and bone, orthopedic fixation devices, and controlled drug-delivery systems [16,17]. Studies showed that blends of polymers with different biodegradable characteristics are an effective measure to provide different pathways for tunable drug release [18,19]. Yet selection and fabrication of biodegradable polymers for appropriate drug release keeps elusive.

As an important biodegradable polymer, PLLA was explored extensively for drug release applications because of its fast hydrolysis [20], however problems persist as how to overcome its brittle feature that usually results in inadequate toughness and low thermal resistance [21]. PCL, an FDA-approved polymer with a low glass transition temperature of −60 °C and remarkable elongation rate at break, is often used with blending of PLLA to improve its toughness [22]. However, PCL has been reported to possess slow hydrolysis [23]. Some studies claimed that melt-blending PLLA with PCL is a feasible way to toughen PLLA while maintaining its biodegradability [24–26]. Thus, the biocompetitive PLLA-PCL composite coatings could therefore be a potential candidate for carrying drugs for appropriate release in the body.

Fabrication of polymer composite coatings can be accomplished via several processing techniques, such as spin coating processing [27], solution electrospinning [28], ultrasonic spraying atomization [29], and dip coating processing [30], etc. Regardless of the ease of operation, there are a number of inherent shortcomings for the abovementioned processing techniques, such as high cost of organic solvents, pronounced toxicity of the residual solvents in the coatings that posed environmental and health issues [31]. To overcome these limitations, alternative coating techniques have to be explored. Among the possible techniques, hot melt method [32], hot melt extrusion [33], and melt electrospinning [34] are basically safe and eco-friendly methods and do not involve the use of solvents. However, for these methods, excessive processing temperatures, high-energy input and low thermal stability and production efficiency are the major concerns. As an alternative processing route, thermal spray offers the advantages of easy operation, cost-efficiency, environmental protection, and have attributes that are beneficial to applications in many fields like drug delivery systems using polymer materials [35,36]. Liquid flame spray processing temperature is the lowest among the thermal spray techniques, which already showed feasibility in fabricating polymer coatings [37,38]. For the processing, the use of water or ethanol as a solvent eliminates many of the shortcomings associated with organic solvent-based coating techniques. Particularly, liquid flame spray usually involves heating the polymers to the temperatures above their melting temperature (T_m) to make uniform coatings. In addition, this processing offers the advantages of incorporating various additives with ease into polymer to fabricate desired composites. Zhou et al. have reported polyimide-alumina composite coatings fabricated by liquid flame spraying [39]. Liu et al. found constrained release of copper from liquid flame sprayed polyimide-copper coatings [40]. Despite the successes of liquid flame spray in depositing polymer coatings, to the best of our knowledge, flame spray construction of biodegradable-polymer based coatings loaded with drugs keeps elusive, and related knowledge of tunable release of drugs from flame sprayed coatings is still lacking.

In this study, chloramphenicol (CAM), a broad-spectrum antibiotic with bacteriostatic activity [41], was used as a model drug for constructing CAM-containing polymer coating deposited by liquid flame spraying. CAM was added in PLLA and PCL as a carrier suspension for subsequent coating fabrication. Physicochemical properties of the coatings were characterized by differential scanning calorimetry (DSC) measurements, scanning electron microscopy (SEM) and X-ray diffraction (XRD), and *in vitro* release profiles have been evaluated. Herein, our study aimed at providing a novel approach towards the preparation of cost-effective and tunable drug delivery coatings as controlled-release materials. These materials have widespread applications for future drug loading and shed light on the design of new drug delivery systems.

Table 1
Sample designation and composition of the composites.

Composition (wt%) PLLA: PCL	Drug-free coating sample code	Drug-loaded coating
		Sample code
100:0	100PLLA	100PLLA-CAM
70:30	70PLLA-30PCL	70PLLA-30PCL-CAM
50:50	50PLLA-50PCL	50PLLA-50PCL-CAM
30:70	30PLLA-70PCL	30PLLA-70PCL-CAM
0:100	100PCL	100PCL-CAM

2. Materials and methods

2.1. Materials and reagents

Commercially available polylactic acid (PLLA-4032D, Nature Works, USA) with an average molecular weight of 50,000 and polycaprolactone (PCL, Nature Works, USA) with an average molecular weight of 80,000 were used. Other reagents and chemicals, sodium chloride, potassium chloride, disodium hydrogen phosphate, potassium dihydrogen phosphate, and chloramphenicol, were purchased from Aladdin (Shanghai, China) and used as received.

2.2. Suspension processing of PLLA-PCL composite

PLLA-PCL composite suspensions with various weight ratios (100/0, 70/30, 50/50, 30/70, and 0/100 wt%) were prepared with a concentration of 10 % (*w*/w) in the mixture of deionized water and ethanol (1:1 *v*/v) and mixed for 1 h with a magnetic stirrer at room temperature. For CAM-loaded samples, 2.5 % (w/w) of CAM powders relative to the total weight of PLLA and PCL were added into the above suspensions. Sample designations and corresponding compositions are listed in Table 1 as below.

2.3. Coating deposition

Coatings were deposited on 316 L stainless steel substrates with the dimension of 25 × 20 × 1 mm (L × W × H) by flame spray (CDS 8000, Castolin, Germany). Prior to the deposition, steel substrates were grit-blasted and ultrasonicated in acetone, ethanol, and deionized water in sequence. The suspensions were injected into the flame with a home-made spray atomizer. Acetylene was used as the fuel gas with a flow rate of 1.5 Nm^3/h and working pressure of 0.1 MPa. Oxygen was used as the combustion-supporting gas with a flow rate of 2.5 Nm^3/h and working pressure of 0.5 MPa. The precursor feed rate of polymer suspension was set as 40 mL/min and the spray distance was 200 mm.

2.4. Characterization of the coatings

Chemistry of the coatings was examined by Fourier transform infrared spectroscopy (FT-IR, Nicolet iS50, Thermo Scientific, USA) operated at a spectral resolution of 4 cm^{-1} with a scan range of 4000–400 cm^{-1} with the highest resolution of 0.09 cm^{-1}. Morphological features of the starting powder and the flame sprayed coatings were characterized by scanning electron microscopy (SEM, Regulus 8230, Hitachi, Japan). Thermal behaviors of the samples were detected using differential scanning calorimetry (DSC 2500, TA Instruments, USA) with a heating rate of 10 °C/min within the temperature range of −70 - 200 °C in nitrogen atmosphere. Melting temperature (T_m),

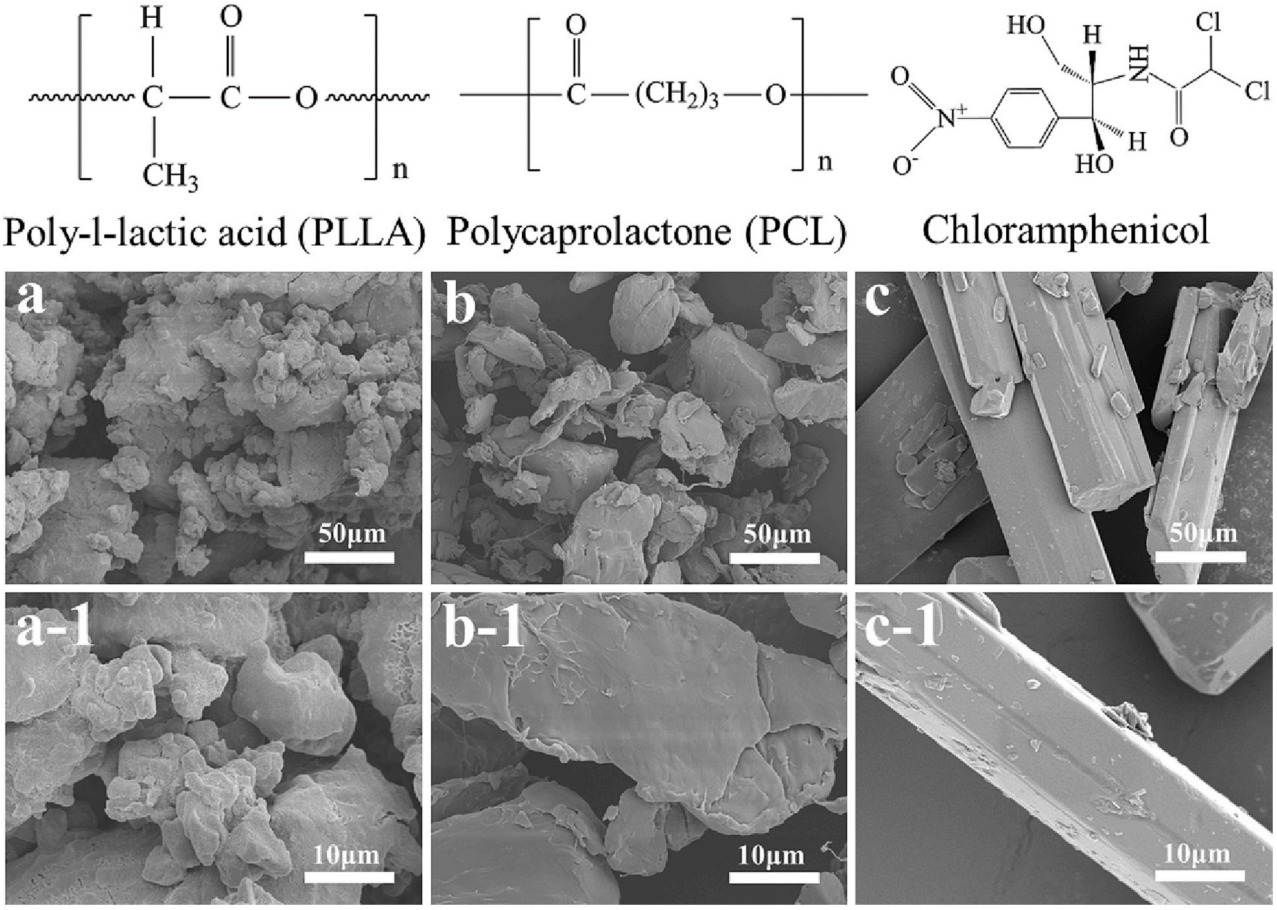

Fig. 1. Depiction of the chemical structure and SEM images of the polymers and drug employed in this study, the corresponding magnified SEM images are shown as (−1). (a, a-1) PLLA powder, (b, b-1) PCL powder, and (c, c-1) CAM powder.

crystallization temperature (T_c), cold crystallization temperature (T_{cc}), and glass transition temperature (T_g) of the PLLA powder, the PCL powder, the CAM powder and the drug-containing composite coating were measured. The following equation was used to calculate the intrinsic degree of crystallinity (X_c) [22]:

$$(X_c)\ \text{Crystallinity}\% = (\Delta H_m)/\left(\Delta H_{\mathrm{m}}^{\circ} \times W_f\right) \times 100 \quad (1)$$

where ΔH_m is the enthalpy of crystallization of each polymer within each sample, W_f represents the weight fraction of each polymer in the sample, ΔH_m refers to the specific melting enthalpy of 100 % crystalline PLLA and PCL, which was reported to be 93 J/g [42] and 135 J/g [43], respectively. The structure of samples was further characterized by X-ray diffraction (XRD, D8 Advance, Bruker, Germany) with a Cu K_α radiation operated at a voltage of 45 kV and a tube current of 40 mA. Samples were scanned at a scan step of 0.015°/s over the 2θ range of 5° - 40°. Vicker's hardness measurements were performed on the samples using a microhardness tester (Wilson, VH3300, USA), with a dwell time of 10 s and an applied force of 0.1 kg. The adhesion strength of the polymer coating was tested using a universal testing machine (MTS, CMT 5205, USA) according to ASTM-C633 standard [44]. 316 stainless steels of 25 × 25 mm^2 were used as substrate of polymer coatings. Samples were glued to the studs using adhesive (ResinLab, EP11HT, USA) and cured for 12 h at 37 °C under a pressure of 10 N. Surface wettability of the composite coatings was evaluated by a water contact angle measurement system (KRUSS, DSA25E, Germany). For the testing, 2 μL of distilled water was dropped onto the coating surface using the sessile drop method before the images were captured by a video camera equipped with the system. For each sample, at least three independent readings acquired at different locations were collected for an average value. For characterization of the size of CAM particles, CAM were dissolved in ethanol, then a small amount of the solution was dropped onto silicon plate, followed by room temperature evaporation of the ethanol. Morphologies of the CAM particles were then characterized by SEM.

2.5. Evaluation of the drug releasing behavior

Releasing behaviors of the CAM loaded in the composite coatings were evaluated in phosphate-buffered saline (PBS) at pH 7.4 using the ultraviolet-visible spectroscopy (Agilent Cary 5000) operated at 278 nm wavelength as previously reported [45]. The CAM-loaded coatings were placed in 50 mL reagent tubes containing 15 mL PBS solution at 37 °C. At different time intervals of 3 h, 6 h, 12 h, 24 h, 48 h, 72 h, 96 h, 168 h, 216 h, 264 h, 312 h, and 360 h, 3 mL of PBS was taken out and replenished with 3 mL of fresh PBS to maintain the same release conditions. To evaluate the drug loading capacity in the polymer coatings, the tested samples were placed in conical flasks containing 15 mL chloroform and underwent magnetic stirring for 4 h at 37 °C. Subsequently, the released CAM was quantified using the UV–Vis spectroscopy. The accumulated quantity of the released CAM was calculated according to the following formula [46]:

$$Q = \left(C_t{*}V + V_i{*}\sum_{i=0}^{t-i} C_i\right) \quad (2)$$

where Q is cumulative total released CAM in ug; C_t is the CAM concentration collected at t time point, mg/mL; V is the volume of released medium, 15 mL PBS in this case; V_i is the volume of the sample taken at

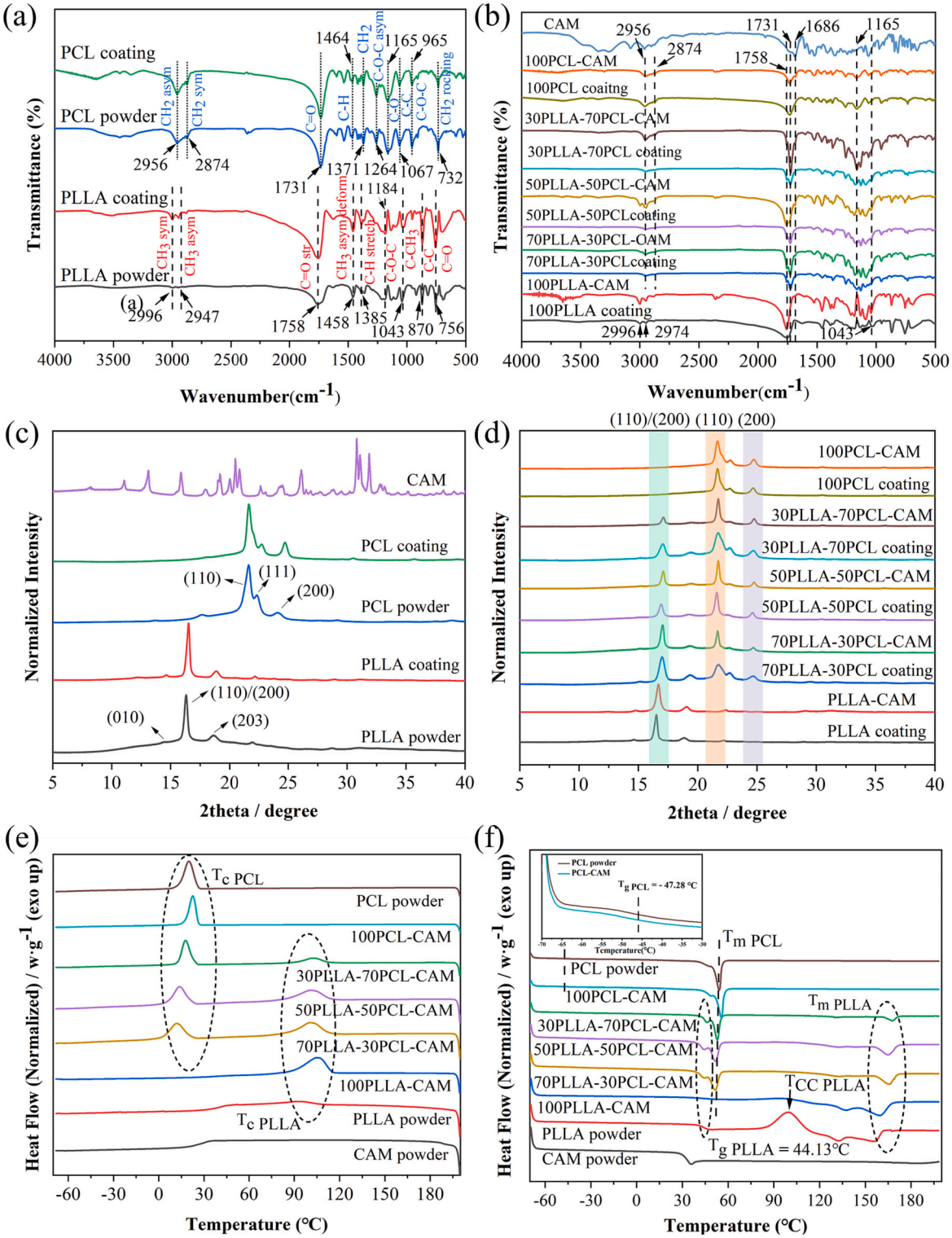

Fig. 2. (a, b) FT-IR spectra, (c, d) XRD patterns and (e, f) DSC curves of PLLA powder, PCL powder, CAM powder, PLLA coating, PCL coating, PLLA-PCL and PLLA-PCL-CAM composite coatings.

each time point ($V_0 = 0$), 3 mL in this case; C_i is the concentration of collected sample per time point ($C_0 = 0$), μg/mL; t is sampling frequency. Each testing was repeated for three replicates and the data collected were treated as mean value ± standard deviation.The percentage of released CAM was calculated based on the formula [14]:

$$\text{Release}\ (\%) = Q_t/Q_\infty \text{X}\ 100 \quad (3)$$

where Q_t is the amount of the released drug at the testing time point t (ug), Q_∞ is the total amount of the drug loaded in the coating (ug). The data was further fitted to the release kinetics models, namely zero order, first order, Higuchi and Korsmeyer-Peppas. The fitting of each model was elucidated based on correlation coefficient (R^2) values. The drug release dynamics were further elucidated using the zero-order model: $Q_t/Q_\infty = K_0 t$, the first-order model: $Ln\,(1 - Q_t/Q_\infty) = -K_1 t$, the

Higuchi model: $Q_t/Q_\infty = K_{HI}t^{0.5}$, and the Korsmeyer-Peppas model: $Q_t/Q_\infty = K_{KP}t^n$ [47,48]. For these equations, Q_t is the amount of the drug released at the time t, Q_∞ is the total amount of the drug in the coating, and Q_t/Q_∞ is equal to the mass fraction of the drug released at the time t, K_0 is the zero-order rate constant expressed in units of concentration/time and t is the time in per unit time, K_1 is first order rate constant, K_{Hi} is the Higuchi's rate constant, K_{KP} is the Higuchi's rate constant and n is the release exponent that characterizes the mechanism of release of tracers. If n is 0.45 or less, the release mechanism corresponds to a Fickian diffusion mechanism, $0.45 < n < 0.89$ means non-Fickian transport or anomalous diffusion [14].

2.6. Antibacterial inhibition assay

Antibacterial activity of the coatings was measured using the agar diffusion method. For the testing, two strains of bacteria, Gram-positive bacteria *Staphylococcus aureus* (CMCC(B)26,069) and Gram-negative bacteria *Escherichia coli* (ATCC25922), were used, which were inoculated in disposable plates with the bacteria concentration of 10^7 to 10^8 colony-forming units (CFU)/mL. The coating samples were placed in 15 mL PBS buffer at 37 °C and 10 μL of the solution were taken out at fixed time intervals (24 h, 120 h), and dropped onto Luria-Bertani (LB) and Tryptone Soybean Broth (TSB) agar plates containing *E. coli* and *S. aureus*, respectively. The plates were left at room temperature for 20 min to allow the agar surface to dry. Drops of pure chloramphenicol solution (0.1 mg/mL) were placed in the same manner on the disposable plates as positive control. A negative control was also examined for all the coatings samples to verify non-antibacterial traits of composites. The sizes of the inhibition zones formed in the bacterial agar plates were measured after 24 h of incubation at 37 °C to evaluate the antibacterial efficacy.

3. Results and discussion

Depictions of the chemical structures and SEM images of the PLLA, the PCL, and the CAM used in this study are shown in Fig. 1. Original PLLA and PCL powders exhibited irregular shapes. Since PLLA and PCL are thermodynamically incompatible systems, mixture of the two materials shows a physical cross-linked network structure that preserves the respective properties of the two polymers. On the other hand, CAM particles were in rod shapes. The antibacterial effect of CAM is realized by inhibiting the synthesis of bacterial protein, which mainly acts on the subunit 50S of bacterial ribosomes, inhibits the transpeptidase reaction of peptide acyltransferase, affects the extension of peptide chain, and produces antibacterial effect [49].

FT-IR spectra of the pure polymers PLLA, PCL, PLLA coating and PCL coating are shown in Fig. 2 and Table S1. FT-IR spectra of the samples show that the main peaks of the pure PLLA powder are located at 2996, 2948, 1758, 1458, 1385, 1184, 1043, 870 and 756 cm^{-1} (Fig. 2a), which are attributed to C—H symmetric stretching vibration, C—H asymmetric stretching vibration, C═O stretch mode, CH_3 asymmetric stretching deform, C—H stretching, C-O-C, C-CH_3, C—C and C═O, respectively [50,51]. For the PCL powder, the characteristic adsorption peaks are clearly seen at 732 cm^{-1} for CH_2 rocking, 965 cm^{-1} for C-O-C, 1067 cm^{-1} for C—C, 1165 cm^{-1} for C—O, 1264 cm^{-1} for C-O-C asymmetric stretching, 1371 cm^{-1} for CH_2, 1464 cm^{-1} for C—H stretching, 1731 cm^{-1} for C═O stretching, and 2956 cm^{-1} for CH_2 asymmetric stretching and 2874 cm^{-1} for symmetric CH_2 stretching, respectively [52]. It is noted that the starting polymer powder and their coatings samples showed the featured FT-IR absorption peaks with minor differences, indicating no chemical structure changes occurred for the polymers during the high temperature coating deposition. In addition, the PLLA-PCL composite coatings display the distinctive FT-IR peaks of C-CH_3 stretching at 1043 cm^{-1}, C═O stretching vibrations at 1758 cm^{-1}, C—H stretching vibrations at 2996 and 2947 cm^{-1}, CH_2 asymmetric stretching and CH_2 symmetric stretching at 2956 and 2874 cm^{-1}, C═O stretching at 1731 cm^{-1}, and C—O stretching at 1165 cm^{-1}. All these peaks are assigned to PLLA and PCL. The strong peak at 1686 cm^{-1} is seen for the FT-IR curve of the PLLA-PCL-CAM composite coating, which refers to the amide group of the drug CAM [41]. It was reported that diminished intensity of the FT-IR peak for the amide group band of the polymer coatings was due to the breakdown of the intermolecular hydrogen bonding and the environment associated with -CONH- stretching changes [41]. These results suggest that CAM has been successfully loaded in the polymer coatings through being physically trapped within the polymer composites.

Table 2
DSC measurement data of the PLLA-PCL composite coating.

Samples	T_c (°C)	ΔH_c ($J{\cdot}g^{-1}$)	T_m (°C)	ΔH_m ($J{\cdot}g^{-1}$)	X_c (%)
PLLA powder	93.0 ± 0.2	4.5 ± 0.4	154.2 ± 2.1	30.7 ± 0.8	32.8
PLLA-CAM	104.8 ± 0.2	36.4 ± 0.1	158.0 ± 1.7	53.8 ± 0.02	57.4
70PLLA-30PCL-CAM[a]	106.3 ± 0.2	25.0 ± 0.4	165.8 ± 0.1	22.5 ± 1.4	34.3
	9.5 ± 0.2	15.8 ± 1.7	51.2 ± 0.04	17.8 ± 1.5	43.9
50PLLA-50PCL-CAM[a]	100.5 ± 0.3	19.6 ± 0.2	165.6 ± 0.5	11.5 ± 0.4	24.5
	12.6 ± 1.4	18.57 ± 0.1	51.50 ± 0.1	19.2 ± 0.3	28.5
30PLLA-70PCL-CAM[a]	101. 8 ± 0.3	14.5 ± 0.2	167.6 ± 0.6	5.8 ± 0.2	20.5
	17.8 ± 0.1	32.2 ± 0.5	52.2 ± 0.6	31.8 ± 1.2	33.7
PCL-CAM	23.1 ± 0.1	50.9 ± 1.5	55.32 ± 0.4	54.9 ± 0.7	40.7
PCL powder	20.2 ± 0.01	52.5 ± 0.4	55.4 ± 2.3	52.3 ± 3.3	38.7

[a] The values on the top within the layer represents the PLLA temperature; whereas the bottom values represent PCL temperature profiles.

XRD detection further evidences the successful incorporation of CAM into the coatings (Fig. 2c). XRD pattern of the PLLA powder exhibits intense diffraction peaks at 14.75° , 16.69° and 19.05°, which are assigned to the planes (010), (110) or (200) and (203) of PLLA, respectively [53]. The PCL powder exhibits two sharp diffraction peaks at 21.65° and 24.05° attributing to the reflections from the (110) and (200) planes, with the shoulder peak at 22.34° assigned to the reflections from the plane (111) [54,55]. Meanwhile, the CAM powder is highly crystalline in nature as intense XRD peaks appear at 11.06°, 13.09°, 20.48°, 30.81° and 31.86° [56]. For the PLLA coating and the PCL coating, there is no big difference in shifting of the XRD peaks as compared to the XRD peak of the starting polymer powder. However, it can be seen in Fig. 2d that no diffraction peaks suggesting crystalline state of CAM are observed in the PLLA-PCL composite coatings. This suggests that CAM drug exists in amorphous form in the polymer coating, which is in agreement with the findings for hydrophobic drugs such as sirolimus, paclitaxel and progesterone in polymer-matrix composites [57–59]. It was claimed that almost complete amorphization of CAM was achieved when CAM content is below 10 wt% in polymer-based blends [60]. In addition, it is noted that the PLLA-PCL-CAM composite coating showed the prominent diffraction peaks without notable shifting as compared with the CAM-free polymer coatings, suggesting that the addition of CAM has no apparent influence on the crystal structure of the composites. This is likely due to the amorphous state of CAM particles in the composites.

Thermal behaviors of the samples were also characterized by DSC (Fig. 2(e-f)). T_c, ΔT_c, T_m, ΔH_m and crystallinity values are listed in Table 2. The PLLA powder has a relatively broad T_c peak at ~93.17 °C, whilst the PCL powder showed T_c of 20.24 °C after annealing. The composite coating of PLLA with PCL altered their inherent individual

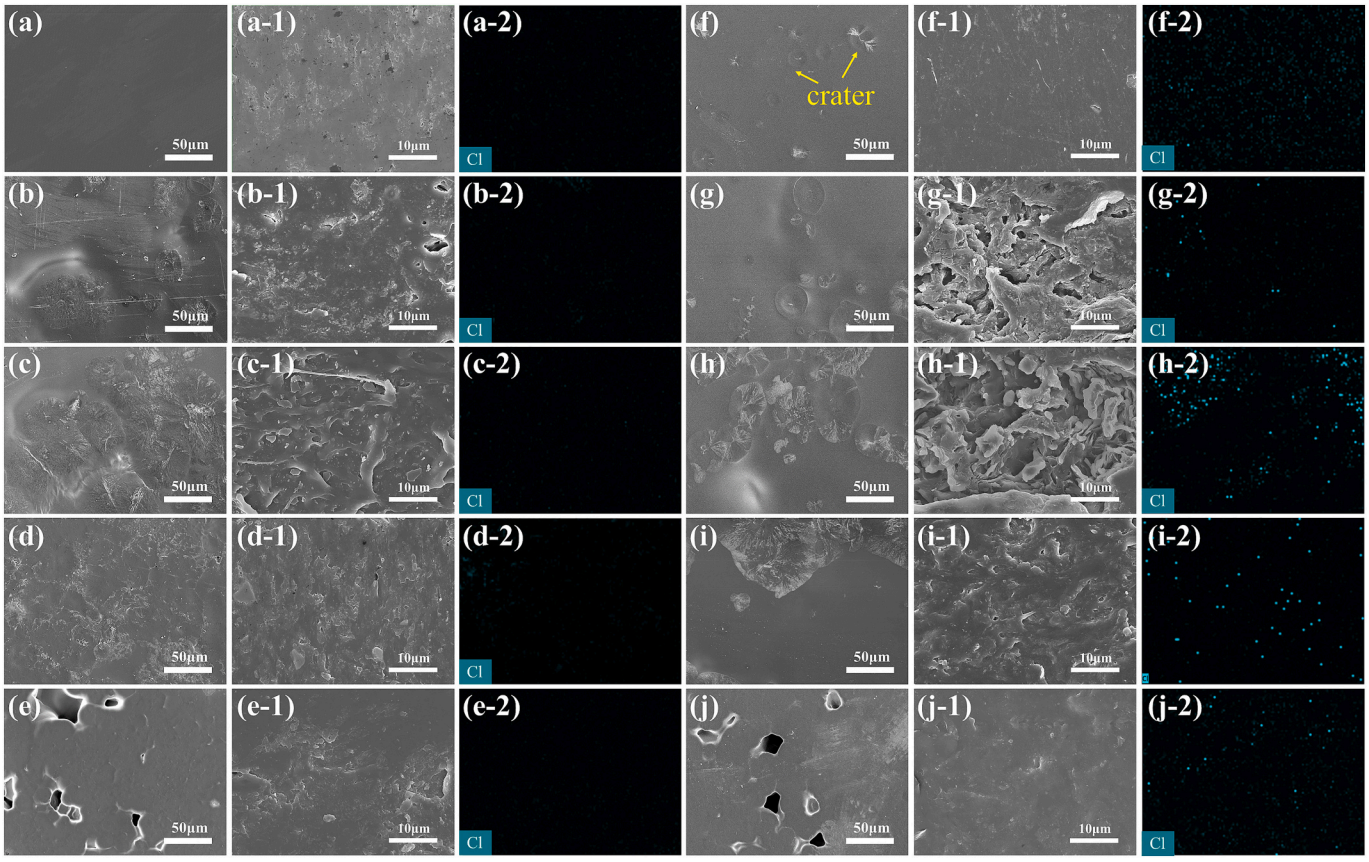

Fig. 3. Surface morphology of the composite coatings, (a) neat PLLA coating, (b)70PLLA-30PCL coating, (c) 50PLLA-50PCL coating, (d) 30PLLA-70PCL coating, (e) neat PCL coating, (f) PLLA-CAM coating, (g) 70PLLA-30PCL-CAM coating, (h) 50PLLA-50PCL-CAM coating, (i) 30PLLA-70PCL-CAM coating, (j)100PCL coating; (−1) SEM images of the fracture surfaces of the corresponding left coatings; (−2) EDS mapping of corresponding the fracture surfaces area.

crystallization behaviors (Fig. 2e). DSC of the PLLA-CAM coatings revealed that its T_c values was about 105 °C. For the 70PLLA-30PCL-CAM, 50PLLA-50PCL-CAM and 30PLLA-70PCL-CAM coatings, the remarkable decreasing of T_c peak presumably was due to the increase in the number of nuclei generated at lower temperatures, induced by the presence of PCL [61]. During the second DSC heating measurement from −70 °C to 200 °C (Fig. 2f), the PLLA powder showed a T_g of 44.13 °C and the PCL powder was −47.28 °C. PLLA exhibits a clear cold-crystallization peak at 99.76 °C. This is likely because the initial crystals in the PLLA powder serve as nucleating agent, in turn facilitating the cold-crystallization. However, it is surprising to note a common feature for both the PLLA-CAM coating and the PLLA-PCL-CAM composite coating that T_c peak of PLLA disappeared during the second-run heating. This should be attributed to the impact of the flame spray processing that this high temperature processing affects the cold-crystallization of PLLA. Under a cooling rate of 10 °C/min, the glass transition temperature of CAM is around 32 °C. Below the T_g of CAM, molecular fluidity freezes and nucleation points are no longer formed, and drug crystallization is inhibited [60]. In addition, it was found that T_m of the PLLA powder and the PCL powder was 154.20 °C and 55.42 °C, respectively. The composite coatings of PLLA, CAM and PCL showed altered T_m, being predominately attributed to the degree of immiscibility between PLLA and PCL. Meanwhile, it is notable as shown in Table 2 that ΔH_m displayed different values for the samples that are consistent with the polymer component content.

In comparison with the PLLA coatings fabricated by electrophoretic deposition [62] and electrochemical polymerization [63], the pure PLLA coating deposited by flame spray displayed smooth and homogeneous topography (Fig. 3a). The PLLA-CAM coating presented similar uniform and smooth surface morphology (Fig. 3f), indicating uniform dispersion of CAM drug in the PLLA coating. No significant morphological changes in the PLLA-CAM coating are seen. However, for the PLLA-CAM coating, as shown in Fig. 3f, craters on its surface are obvious, which are likely formed during the melting to crystallizing stage of PLLA as a result of contraction of its molecular chain after crystallization [64]. For the pristine PLLA-PCL composite coatings and PLLA-PCL-CAM composite coatings, their SEM images shown in Fig. 3(b-d, j-i) evidenced the "sea-island" phase of polymer blending, which was also reported by Guan et al. [65]. Clearly, the properties of each matrix component, the processing conditions and their internal posture structures affect macroscopic properties of polymer blends [66,67]. Interestingly, the PCL-CAM coating showed more pronounced porous structure than the PLLA-CAM coating (Fig. 3j), and this might be due to the different evaporation rates of deionized water and ethanol. Ethanol volatilizes more rapidly than water under the high temperature flame spray processing, giving rise to a more porous structure through the volatilization of water [68–70]. Under the same flame spray conditions, the PLLA-CAM coating showed smooth pore-free surface, for the viscosity of PLLA is lower than that of PCL. Lower viscosity usually means better fluidity [71]. Taking advantage of abovementioned features of PCL, PCL nanofibrous scaffolds with hierarchical pores and PCL porous microspheres were synthesized and characterized by other research teams [72,73]. Furthermore, the morphology of the cross-sections of the coatings was characterized by SEM imaging. The images show flatcross-sectional morphologies of both the PLLA and the PLLA-CAM coatings (Fig. 3(a-1, e-2, f-1, j-2)), being similar to the PCL and the PCL-CAM coatings. The results indicate that the addition of CAM has no remarkable effect on the internal structure of the coatings. Compared to single polymer coating, however, the image of PLLA-PCL composite coating presented in Fig. 3(b-1, c-1, d-1, g-1, h-1, i-1) reveals phase-separated morphology, indicating poor compatibility

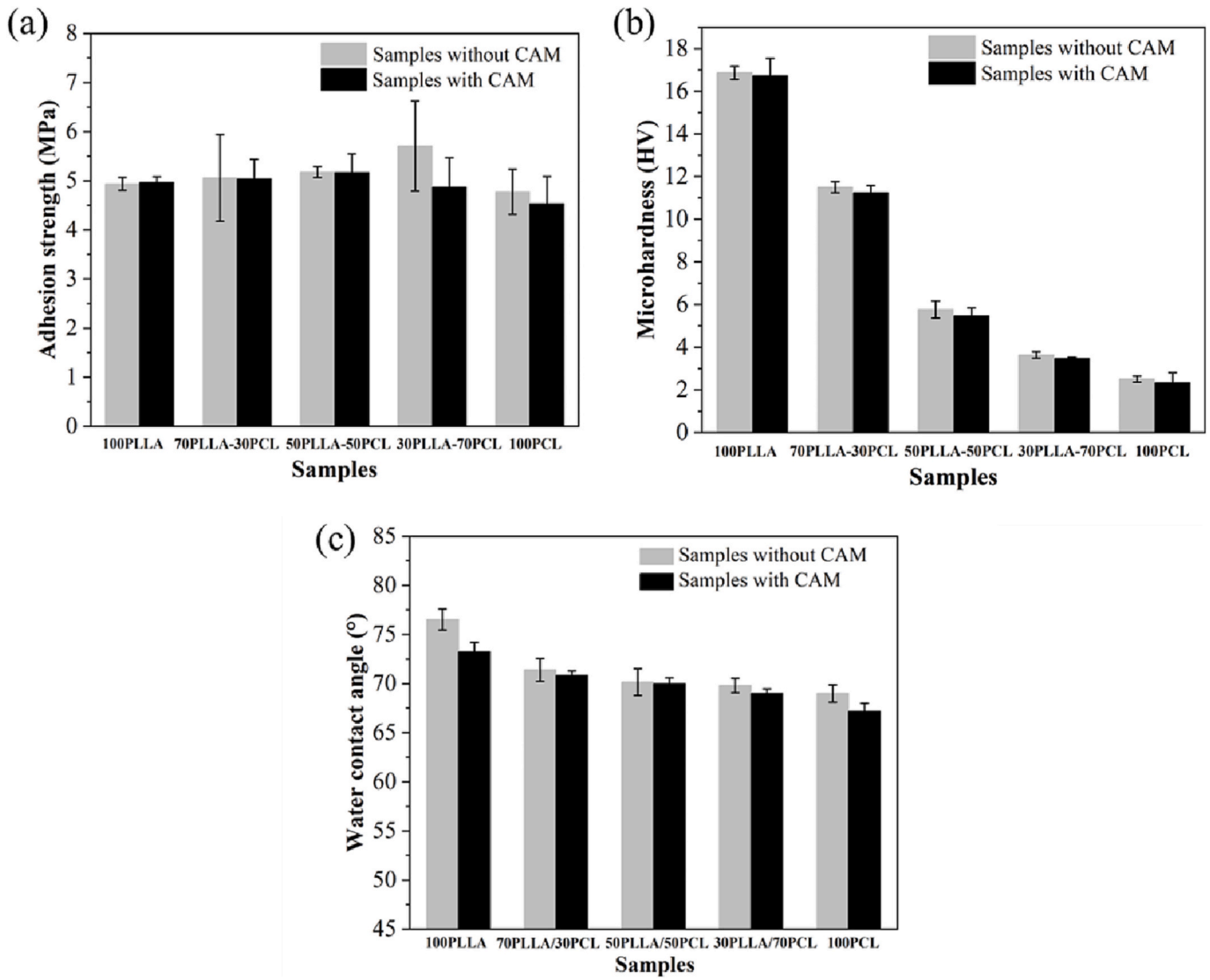

Fig. 4. (a) Adhesion strength, (b) Microhardness data and (c) Water contact angle of the drug-free and drug-loaded PLLA-PCL composite coatings with different ratio.

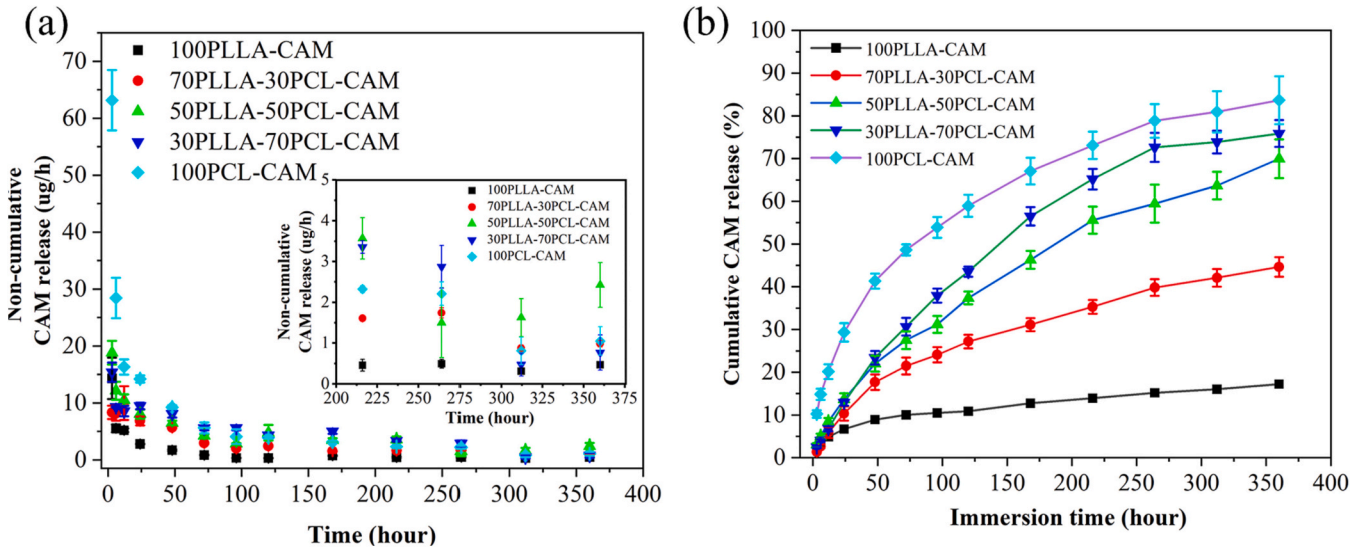

Fig. 5. The non-cumulative (a) and cumulative (b) release behaviors of CAM from the composite coatings.

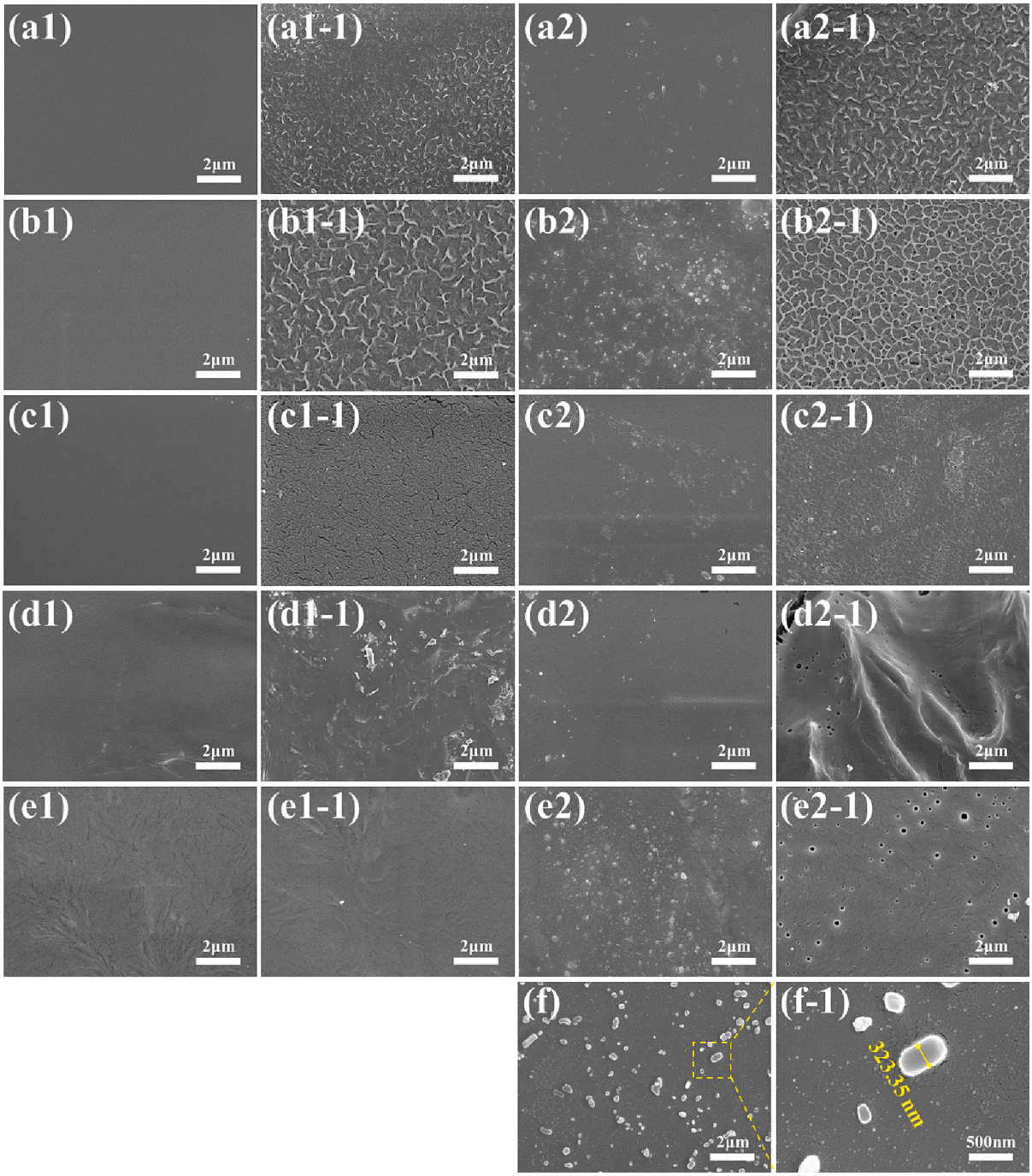

Fig. 6. Surface morphologies of the CAM-free coatings and the CAM-containing coatings with different ratios exposed to the PBS solution after 0 day and 15 days, (a1, b1, c1, d1, e1) 100PLLA, 30PLLA-70PCL, 50PLLA-50PCL, 30PLLA-70PCL and 100PCL coating, (a2, b2, c2, d2, e2) 100PLLA-CAM, 30PLLA-70PCL-CAM, 50PLLA-50PCL-CAM, 30PLLA-70PCL-CAM and 100PCL-CAM coating after 0 day and (−1) after 15 days release testing in PBS; (f, f-1) SEM pictures showing the CAM particles after evaporation on silicone plate.

between PLLA and PCL, thus immiscible characteristics [67]. EDS detection shows presence of Cl within the CAM-loaded coating (Fig. 3(f-2, i-2, j-2, k-2, l-2)), suggesting well dispersion of the drug CAM inside.

The adhesion and microhardness of the drug-free and drug-loaded PLLA-PCL composite coatings were studied and shown in Fig. 4. It can be seen that there is no significant difference in adhesion among the drug-free and drug-loaded coatings, suggesting excellent consistence of the flame spray process (Fig. 4(a)). Fig. 4(b) shows the microhardness of the PLLA coating, PCL coating and the composite system. It is obvious that the microhardness of the PLLA coatings was much higher than that of the PCL coating, and the microhardness of the PLLA-PCL composite coatings decreased with the content of PCL. In addition, the incorporation of drugs did not result in significant change in the microhardness compared with the drug-free counterparts. Surface wettability of the coatings was further assessed using the sessile drop method, since it participates in regulating interaction of the coatings with microorganisms contacting their surfaces [74]. The water contact angle values of the coatings with/without CAM are presented in Fig. 4(c). The contact angle is 76.52° ± 1.08° for the PLLA coating and 73.22° ± 0.99° for the PLLA-CAM coating. This is not surprising since CAM is hydrophilic in nature. The wettability values are consistent with other studies on poly (L-lactide) [75,76]. The slight changes in wettability caused by the

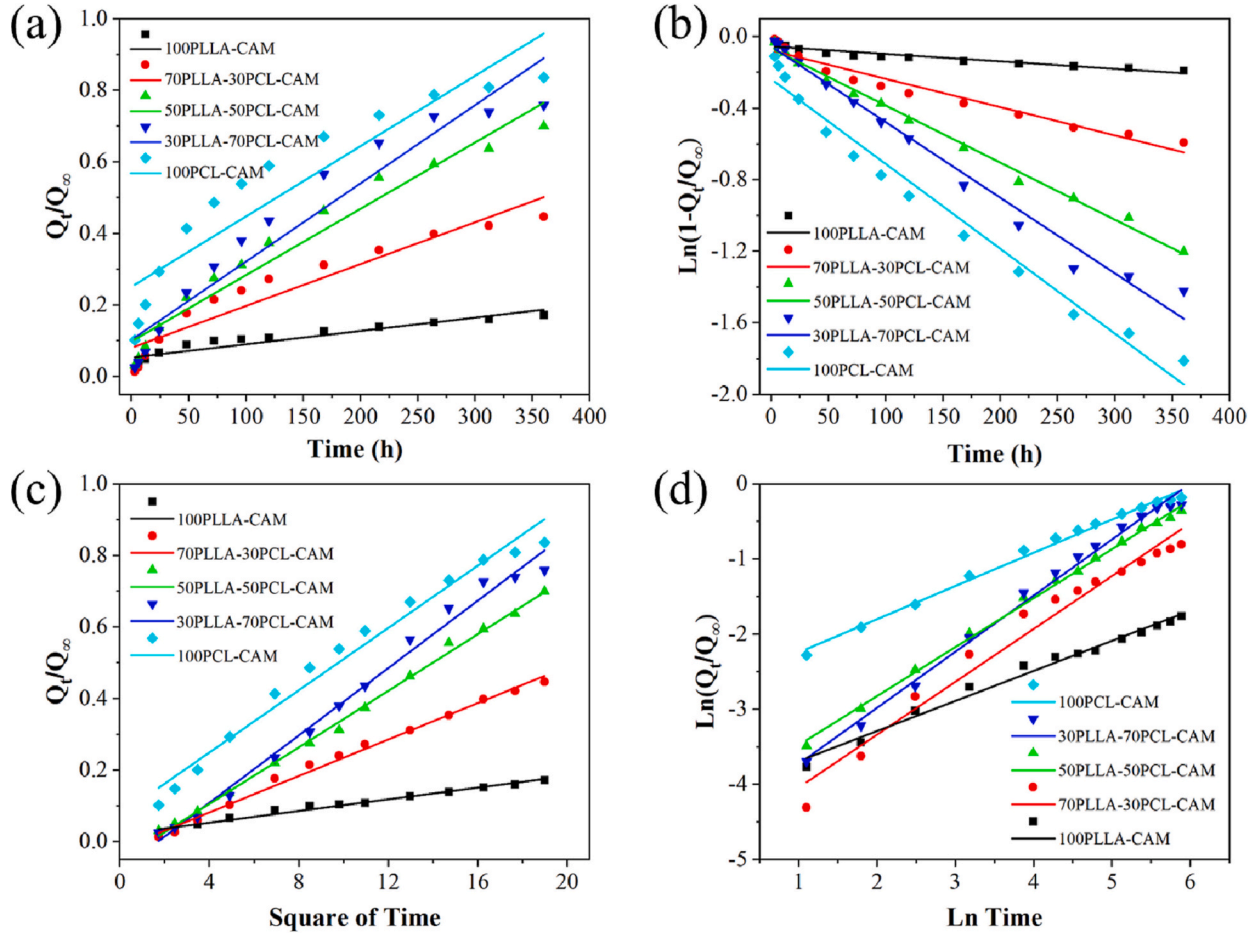

Fig. 7. Characteristics of the drug release behaviors of the CAM-containing coatings by applying the Zero-order model (a), the first-order model (b), the Higuchi model (c), and the Korsmeyer-Peppas model (d).

addition of CAM would be beneficial to prevent non-specified protein adsorption and platelet adhesion [77].

The drug release behaviors of the fabricated coatings were then analyzed. As shown in Fig. 5(a), all the coatings showed quick release of CAM at the starting hours, which is likely due to its extensive concentration gradient on their surfaces, and then sustained slow release over the duration of the experiment. The sample without PCL, i.e. 100PLLA-CAM, showed the minimum CAM release and the amount of released CAM increased with the increase of PCL content in the coating. It can be seen from Fig. 5(b) that 6.71 ± 0.60 %, 10.34 ± 1.67 %, 13.63 ± 1.41 %, 12.92 ± 0.75 % and 29.35 ± 2.15 % of CAM were released at 100PLLA-CAM , 70PLLA-30PCL-CAM, 50PLLA-50PCL-CAM, 30PLLA-70PCL-CAM and 100PCL-CAM coating, respectively, in one day. The release of CAM from the PLLA-CAM coating is significantly slower than that of the PCL-CAM coating during the whole release time. This is presumably because the PLLA-CAM coating has more pronounced hydrophobic structure owing to the presence of larger aliphatic hydrocarbon chains. The PCL-CAM coating with hydrophilicity and porous structure showed remarkably fast releasing of CAM. As shown in above DSC analysis (Fig. 2(f)), PCL is a semi-crystalline polymer with a T_g of -47.28 °C while PLLA is an amorphous polymer with a T_g of 44.13 °C. The PCL backbone chain is presumed to be in a highly flexible state at 37 °C and therefore free volume can well swell well and releases drug relatively easily. On the contrary, the entanglement of the molecular chains makes the movement of the PLLA chains difficult, which limits the drug release rate. The release performance of PLLA-PCL-CAM composite coatings can be ascribed to the combined effect of PLLA and PCL polymer. Our finding is consistent with the release profiles of naproxen sodium from electrospun-aligned PLLA-PCL scaffolds reported by Lui et al. [78].

To further understand the release behaviors of CAM, surface morphologies of the drug-free and drug-loaded coatings with different ratio

Table 3
The variables calculated from the release kinetics of CAM.

Samples		100PLLA-CAM	70PLLA-30PCL-CAM	50PLLA-50PCL-CAM	30PLLA-70PCL-CAM	100PCL-CAM
Zero-order model	K_0 (*10^{-4})	3.72	11.70	18.50	21.90	19.70
	R^2	0.877	0.903	0.951	0.923	0.857
First-order model	K_1 (*10^{-3})	−0.42	−1.58	−3.19	−4.23	−4.74
	R^2	0.893	0.946	0.993	0.981	0.975
Higuchi model	K_{HI} (*10^{-2})	0.815	2.55	3.95	4.71	4.35
	R^2	0.979	0.992	0.997	0.989	0.978
Korsmeyer-Peppas model	K_{KP} (*10^{-2})	1.68	1.58	1.62	1.14	6.80
	R^2	0.985	0.968	0.997	0.992	0.992
	n	0.400	0.703	0.652	0.747	0.442

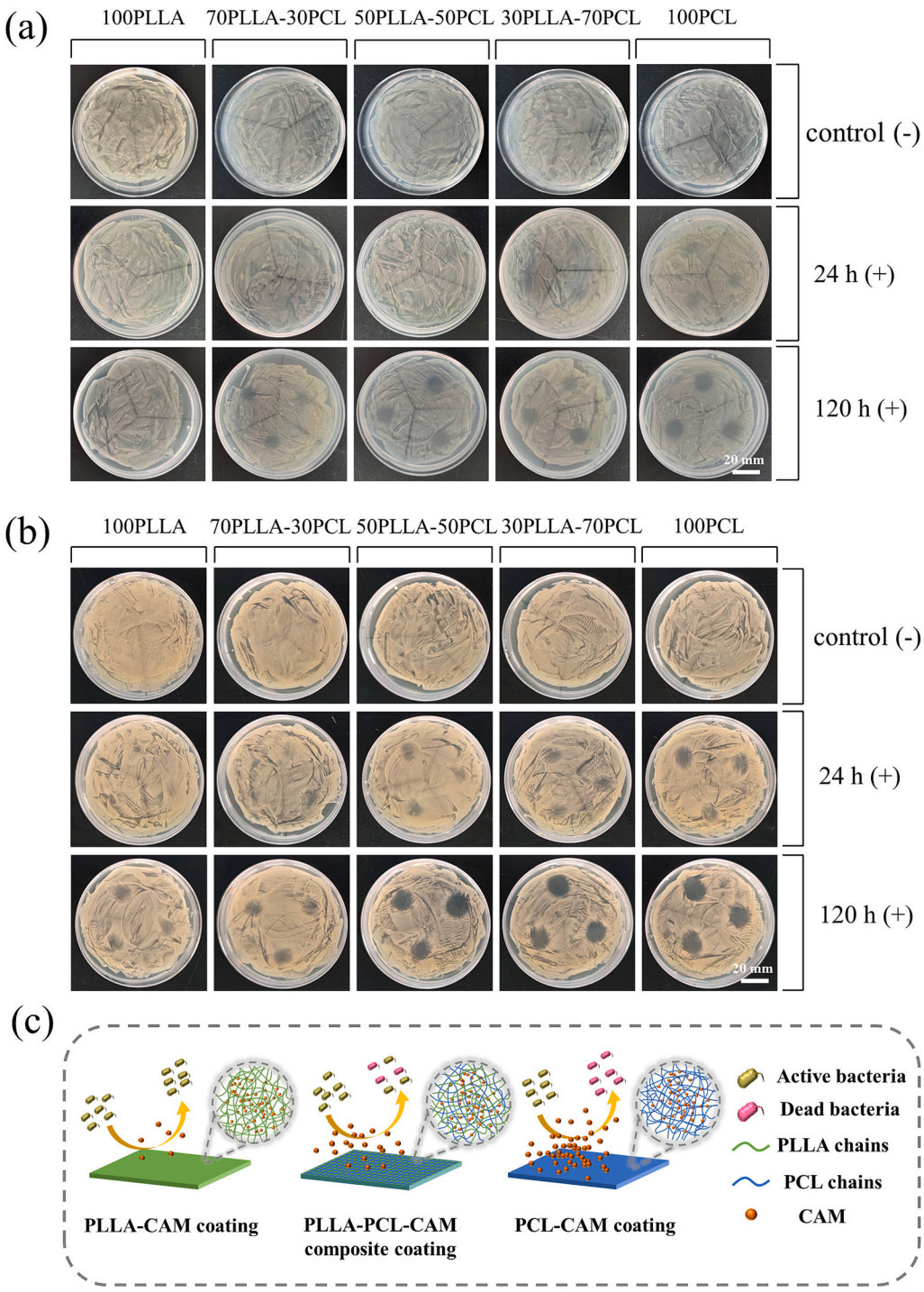

Fig. 8. Digital images of inhibition zones created after pouring on agar plates with *E. coli* (a) and *S. aureus* (b) 10 μL drops of the leachates obtained from PLLA-PCL composite coatings: (−) composite coating without CAM and (+) composite coating containing CAM. (c) Schematic diagram for drug release and antibacterial effect of different composite coatings.

of PLLA and PCL were characterized after 15 days incubation in PBS. The releasing of CAM from CAM-loaded coatings is clearly seen as evidenced by the pores located on their surfaces (Fig. 6). To confirm the fact that the pores were induced by CAM release, the size of the drug particles was characterized separately by SEM (Fig. 6(f, f-1)). CAM particles showed an irregular shape with the particle size of <323.35 nm, which matches very well the size of the holes seen on the surfaces of the coatings after drug releasing. This nevertheless proves the continuous releasing of CAM from the coatings. Furthermore, it was noted that the surface-pore density of the CAM-loaded coatings with 100 % or 70 % PCL is higher than that of the coatings with 50 % or 30 % PCL, this in turn suggests that the release of CAM can be tuned by adjusting the percentage of PCL in the PLLA-PCL composite coatings.

The dynamics data are fitted with four commonly used drug release models (Fig. 7(a-d)) and listed in Table 3. It is noted that for the 100PLLA-CAM and the 100PCL-CAM coatings, the drug release fitted the Korsmeyer-Peppas model with the highest linearity correlation coefficient (R^2 = 0.985, 0.992). The release exponent *n* for both of them was ≤0.45, suggesting the drug release mechanism to follow Fick's laws of diffusion. However, changing the polymer mass ratios of the PLLA and

PCL in the composite coatings also altered the release kinetics. The drug release of the 70PLLA-30PCL-CAM coating was best interpreted by the Higuchi's equation ($R^2 = 0.992$), indicating that the drug diffused from the insoluble matrix to the solution at a relatively slower rate. On the contrary, the drug release of the 30PLLA-70PCL-CAM coating fits the Korsmeyer-Peppas model with an R^2 value of 0.992. Moreover, the 50PLLA-50PCL-CAM coating agrees well with both the Higuchi model and Korsmeyer-Peppas model with a same R^2 value of 0.997, further confirming the transition of release mechanism as increasing PCL content in the composite coatings. Furthermore, the release exponent *n* for the 50PLLA-50PCL-CAM and the 30PLLA-70PCL-CAM coatings were higher than 0.45, indicating combined release regimes of erosion and diffusion, named non-Fickian transport. Interestingly, the releasing of drugs from polymer mixtures produced by various fabrication techniques usually follows a specific model and does not show the transition process between release mechanisms. Li et al. [19] reported the Korsmeyer-Peppas model of the drug release from a series of ultrasonic sprayed PDLLA-PLCL blend films with different ratios of PLCL. Liu et al. [79] found that the release curve of CPFX-PCL-PGA coatings conforms to the Ritger-Peppas model. Nevertheless, the release model of our PLLA-PCL-CAM coatings deposited by flame spraying exhibits the features of the initial Korsmeyer-Peppas model, subsequently Higuchi model, and then Korsmeyer-Peppas model, depending on the content of PCL in the coatings. This on the other hand suggests the controllable manner of the drug release, which can be achieved by altering the relative content of PCL in the PLLA-PCL-CAM coatings. These results make it possible that by taking into account the relevant pharmaceutical requirement, such as the maximum release rate and the dissolution efficiency of drugs [80], drug-loaded composite coating formulation can be easily designed. Our findings are inspiring since by using the flame spray processing route, the PLLA-PCL composite coatings offer potential options to design the drug delivery systems with different drug release mechanisms through altering the percentages of either PLLA or PCL in the starting powder.

The ultimate purpose of tailoring the structure of the CAM-containing polymer coatings was to accomplish long-term bactericidal performances. Their anti-microbial performances were assessed using the bacteria *E. coli* and *S. aureus* (Fig. 8). The CAM-free PLLA-PCL coatings were used as the negative control and no inhibition activity against the bacteria was observed. For the CAM-containing coatings, it is notable that their antibacterial activities clearly increase with the content of PCL in composite coatings, and elongated incubation triggered enhanced antibacterial performances for all the CAM-containing coatings. This agrees well with our previous testing result that continuous release of CAM from the coatings with different speed was detected (Fig. 5). These on the other hand imply the feasibility of regulating the release rate of CAM through altering the concentration of PCL in the PLLA - PCL composite coatings. As shown in Fig. 8(c), the release of CAM in a controllable manner from the PLLA-PCL composite coatings gives encouraging insight into design and construction of polymer coatings for long-term antibacterial applications.

4. Conclusions

The PLLA-PCL-CAM composite coatings were successfully fabricated by flame spray technique. The *in vitro* release profiles of CAM from PLLA-PCL composite coatings with different ratios of PCL showed significant dependence of the release behaviors on the content of PCL in the coatings. The physicochemical features of the PLLA-PCL composite coatings were not affected by the addition of the drug. The CAM release data were better fitted with the Higuchi and the Korsmeyer-Peppas models, and the drug release followed the Fick's laws of diffusion in the PLLA-CAM composite coating and the PCL-CAM composite coating. The 70PLLA-30PCL-CAM coating followed the Higuchi model, and the release of CAM was closely related to the drug diffusion distance. The 50PLLA-50PCL-CAM coating well fitted both the Higuchi model and the Korsmeyer-Peppas model, and for the 30PLLA-70PCL-CAM coating, drug release was controlled by anomalous diffusion mechanism. Modulation of the drug release can be achieved by altering the ratio of PLLA to PCL in the composites. The agar diffusion test against *E. coli* and *S. aureus* further suggested that CAM can be released in a controllable way from the PLLA-PCL composite coatings through changing the content of PCL. Our results shed light on potential applications of the flame sprayed drug-loaded coatings for their cost-efficiency, ease of large-scale coating fabrication, and controllable drug release behaviors.

Supplementary data to this article can be found online at https://doi.org/10.1016/j.porgcoat.2023.107807.

CRediT authorship contribution statement

Yonghong Pan: Methodology, Investigation, Writing – original draft, Software. **Daofeng Zhou:** Investigation. **Tingting Cui:** Methodology, Investigation. **Yu Zhang:** Software. **Lei Ye:** Investigation. **Ye Tian:** Methodology, Investigation. **Ping Zhou:** Software. **Yi Liu:** Writing – review & editing, Funding acquisition. **Hidetoshi Saitoh:** Writing – review & editing. **Botao Zhang:** Conceptualization, Writing – review & editing, Supervision, Funding acquisition. **Hua Li:** Writing – review & editing, Funding acquisition.

Declaration of competing interest

The authors declare that they have no known competing financial interests or personal relationships that could have appeared to influence the work reported in this paper.

Data availability

No data was used for the research described in the article.

Acknowledgements

This research was supported by Zhejiang Basic Public Welfare Research Program Project (No. LGF20C100001), National Natural Science Foundation of China (No. 41706076, 52071329), Chinese Academy of Sciences Key Project (ZDRW-CN-2019-3), the Youth Innovation Promotion Association of the Chinese Academy of Sciences, China (No. 2020299), and S&T Innovation 2025 Major Special Program of Ningbo (No. 2018B10054, 2020Z095), and K.C. Wong Education Foundation (No. GJTD-2019-13).

References

[1] N. Kamaly, B. Yameen, J. Wu, O.C. Farokhzad, Degradable controlled-release polymers and polymeric nanoparticles: mechanisms of controlling drug release, Chem. Rev. 116 (2016) 2602–2663, https://doi.org/10.1021/acs.chemrev.5b00346.

[2] P. Davoodi, L.Y. Lee, Q. Xu, V. Sunil, Y. Sun, S. Soh, C.H. Wang, Drug delivery systems for programmed and on-demand release, Adv. Drug Deliv. Rev. 132 (2018) 104–138, https://doi.org/10.1016/j.addr.2018.07.002.

[3] T.T. Nguyen, N.S.N. Saipul Bahri, A.M. Rahmatika, K.L.A. Cao, T. Hirano, T. Ogi, Rapid indomethacin release from porous pectin particles as a colon-targeted drug delivery system, ACS Appl. Bio. Mater. (2023), https://doi.org/10.1021/acsabm.3c00218.

[4] A. Schudel, A.P. Chapman, M.K. Yau, C.J. Higginson, D.M. Francis, M. P. Manspeaker, A.R.C. Avecilla, N.A. Rohner, M.G. Finn, S.N. Thomas, Programmable multistage drug delivery to lymph nodes, Nat. Nanotechnol. 15 (2020) 491–499, https://doi.org/10.1038/s41565-020-0679-4.

[5] W. Zhou, Y. Li, J. Yan, P. Xiong, Q. Li, Y. Cheng, Y. Zheng, Construction of self-defensive antibacterial and osteogenic agnps/gentamicin coatings with chitosan as nanovalves for controlled release, Sci. Rep. 8 (2018) 13432, https://doi.org/10.1038/s41598-018-31843-2.

[6] Y.C. Chen, S. Shishikura, D.E. Moseson, A.J. Ignatovich, J. Lomeo, A. Zhu, S. D. Horava, C.A. Richard, K. Park, Y. Yeo, Control of drug release kinetics from hot-melt extruded drug-loaded polycaprolactone matrices, J. Control. Release 359 (2023) 373–383, https://doi.org/10.1016/j.jconrel.2023.05.049.

[7] S. Petralito, P. Paolicelli, M. Nardoni, A. Tedesco, J. Trilli, L. Di Muzio, S. Cesa, M. A. Casadei, A. Adrover, Gelation of the internal core of liposomes as a strategy for stabilization and modified drug delivery ii. Theoretical analysis and modelling of

in-vitro release experiments, Int. J. Pharm. 585 (2020), 119471, https://doi.org/10.1016/j.ijpharm.2020.119471.
[8] N. Li, W. Lu, J. Yu, Y. Xiao, S. Liu, L. Gan, J. Huang, Rod-like cellulose nanocrystal/cis-aconityl-doxorubicin prodrug: a fluorescence-visible drug delivery system with enhanced cellular uptake and intracellular drug controlled release, Mater. Sci. Eng. C Mater. Biol. Appl. 91 (2018) 179–189, https://doi.org/10.1016/j.msec.2018.04.099.
[9] S.A. Al Jabbar, V. Atiroglu, R.M. Hameed, G.G. Eskiler, A. Atiroglu, A.D. Ozkan, M. Ozacar, Fabrication of dopamine conjugated with protein @metal organic framework for targeted drug delivery: a biocompatible ph-responsive nanocarrier for gemcitabine release on mcf7 human breast cancer cells, Bioorg. Chem. 118 (2022), 105467, https://doi.org/10.1016/j.bioorg.2021.105467.
[10] R. Parhi, Drug delivery applications of chitin and chitosan: a review, Environ. Chem. Lett. 18 (2020) 577–594, https://doi.org/10.1007/s10311-020-00963-5.
[11] S.K. Prajapati, A. Jain, A. Jain, S. Jain, Biodegradable polymers and constructs: a novel approach in drug delivery, Eur. Polym. J. 120 (2019), https://doi.org/10.1016/j.eurpolymj.2019.08.018.
[12] K.J. Hogan, A.G. Mikos, Biodegradable thermoresponsive polymers: applications in drug delivery and tissue engineering, Polymer 211 (2020), https://doi.org/10.1016/j.polymer.2020.123063.
[13] L. Zhou, G. Zhao, W. Jiang, Mechanical properties of biodegradable polylactide/poly(ether-block-amide)/thermoplastic starch blends: effect of the crosslinking of starch, J. Appl. Polym. Sci. 133 (2016) n/a–n/a, https://doi.org/10.1002/app.42297.
[14] M. Ebrahimifar, M. Taherimehr, Evaluation of in-vitro drug release of polyvinylcyclohexane carbonate as a co2-derived degradable polymer blended with pla and pcl as drug carriers, J. Drug Deliv. Sci. Technol. 63 (2021), https://doi.org/10.1016/j.jddst.2021.102491.
[15] W.J. Chong, S. Shen, Y. Li, A. Trinchi, D. Pejak, I. Kyratzis, A. Sola, C. Wen, Additive manufacturing of antibacterial pla-zno nanocomposites: benefits, limitations and open challenges, J. Mater. Sci.Technol. 111 (2022) 120–151, https://doi.org/10.1016/j.jmst.2021.09.039.
[16] X. Yu, W. Huang, D. Zhao, K. Yang, L. Tan, X. Zhang, J. Li, M. Zhang, S. Zhang, T. Liu, B. Wu, M. Qu, R. Duan, Y. Yuan, Study of engineered low-modulus mg/plla composites as potential orthopaedic implants: an in vitro and in vivo study, Colloids Surf. B Biointerfaces 174 (2019) 280–290, https://doi.org/10.1016/j.colsurfb.2018.10.054.
[17] V. Vilay, M. Mariatti, Z. Ahmad, K. Pasomsouk, M. Todo, Improvement of microstructures and properties of biodegradable plla and pcl blends compatibilized with a triblock copolymer, Mater. Sci. Eng. A 527 (2010) 6930–6937, https://doi.org/10.1016/j.msea.2010.07.079.
[18] B. Yu, L. Meng, S. Fu, Z. Zhao, Y. Liu, K. Wang, Q. Fu, Morphology and internal structure control over pla microspheres by compounding plla and pdla and effects on drug release behavior, Colloids Surf. B Biointerfaces 172 (2018) 105–112, https://doi.org/10.1016/j.colsurfb.2018.08.037.
[19] F. Li, X. Li, R. He, J. Cheng, Z. Ni, G. Zhao, Preparation and evaluation of poly(d, l-lactic acid)/poly(l-lactide-co-ε-caprolactone) blends for tunable sirolimus release, Colloid Surf. A-Physicochem. Eng. Asp. 590 (2020), https://doi.org/10.1016/j.colsurfa.2020.124518.
[20] L.N. Woodard, M.A. Grunlan, Hydrolytic degradation of pcl-plla semi-ipns exhibiting rapid, tunable degradation, ACS Biomater Sci. Eng. 5 (2019) 498–508, https://doi.org/10.1021/acsbiomaterials.8b01135.
[21] N.A. Lockwood, R.W. Hergenrother, L.M. Patrick, S.M. Stucke, R. Steendam, E. Pacheco, R. Virmani, F.D. Kolodgie, B. Hubbard, In vitro and in vivo characterization of novel biodegradable polymers for application as drug-eluting stent coatings, J. Biomater. Sci.-Polym. Ed. 21 (2010) 529–552, https://doi.org/10.1163/156856209X429175.
[22] O.J. Botlhoko, J. Ramontja, S.S. Ray, A new insight into morphological, thermal, and mechanical properties of melt-processed polylactide/poly(ε-caprolactone) blends, Polym. Degrad. Stab. 154 (2018) 84–95, https://doi.org/10.1016/j.polymdegradstab. 2018.05.025.
[23] B. Lu, G.-X. Wang, D. Huang, Z.-L. Ren, X.-W. Wang, P.-L. Wang, Z.-C. Zhen, W. Zhang, J.-H. Ji, Comparison of pcl degradation in different aquatic environments: effects of bacteria and inorganic salts, Polym. Degrad. Stab. 150 (2018) 133–139, https://doi.org/10.1016/j.polymdegradstab. 2018.02.002.
[24] H. Liu, J. Zhang, Research progress in toughening modification of poly(lactic acid), J. Polym. Sci. Polym. Phys. 49 (2011) 1051–1083, https://doi.org/10.1002/polb.22283.
[25] G.X. Chen, H.S. Kim, E.S. Kim, J.S. Yoon, Compatibilization-like effect of reactive organoclay on the poly(l-lactide)/poly(butylene succinate) blends, Polymer 46 (2005) 11829–11836, https://doi.org/10.1016/j.polymer.2005.10.056.
[26] J.B. Zeng, Y.D. Li, Y.S. He, S.L. Li, Y.Z. Wang, Improving flexibility of poly(l-lactide) by blending with poly(l-lactic acid) based poly(ester-urethane): morphology, mechanical properties, and crystallization behaviors, Ind. Eng. Chem. Res. 50 (2011) 6124–6131, https://doi.org/10.1021/ie102422q.
[27] E. Albarahmieh, M. Albarahmieh, B.A. Alkhalidi, Fabrication of hierarchical polymeric thin films by spin coating toward production of amorphous solid dispersion for buccal drug delivery system: preparation, characterization, and in vitro release investigations, J. Pharm. Sci. 107 (2018) 3112–3122, https://doi.org/10.1016/j.xphs.2018.08.019.
[28] A. Benk, D. Güçlü, A. Coban, Economical method for producing nascent iodine products with aprotic solvents (nmp, dmso) possessing highly effective antimicrobial properties, J. Polym. Environ. 30 (2021) 1118–1126, https://doi.org/10.1007/s10924-021-02270-8.
[29] H.S. Liu, W.C. Chang, C.Y. Chou, B.C. Pan, Y.S. Chou, G.S. Liou, C.L. Liu, Controllable electrochromic polyamide film and device produced by facile ultrasonic spray-coating, Sci. Rep. 7 (2017) 11982, https://doi.org/10.1038/s41598-017-11862-1.
[30] P. Chinavinijkul, K. Riansuwan, P. Kiratisin, S. Srisang, N. Nasongkla, Dip- and spray-coating of schanz pin with pla and pla nanosphere for prolonged antibacterial activity, J. Drug Deliv. Sci. Technol. 65 (2021), https://doi.org/10.1016/j.jddst.2021.102667.
[31] S. Bose, R.H. Bogner, Solventless pharmaceutical coating processes: a review, Pharm. Dev. Technol. 12 (2007) 115–131, https://doi.org/10.1080/10837450701212479.
[32] Y. Yang, L. Shen, J. Li, W.G. Shan, Preparation and evaluation of metoprolol tartrate sustained-release pellets using hot melt extrusion combined with hot melt coating, Drug Dev. Ind. Pharm. 43 (2017) 939–946, https://doi.org/10.1080/03639045.2017.1287715.
[33] S. Tambe, D. Jain, Y. Agarwal, P. Amin, Hot-melt extrusion: highlighting recent advances in pharmaceutical applications, J. Drug Deliv. Sci. Technol. 63 (2021), https://doi.org/10.1016/j.jddst.2021.102452.
[34] T.D. Brown, P.D. Dalton, D.W. Hutmacher, Melt electrospinning today: an opportune time for an emerging polymer process, Prog. Polym. Sci. 56 (2016) 116–166, https://doi.org/10.1016/j.progpolymsci.2016.01.001.
[35] A. Chebbi, J. Stokes, Thermal spraying of bioactive polymer coatings for orthopaedic applications, J. Therm. Spray Technol. 21 (2012) 719–730, https://doi.org/10.1007/s11666-012-9764-z.
[36] J. Cizek, J. Matejicek, Medicine meets thermal spray technology: a review of patents, J. Therm. Spray Technol. 27 (2018) 1251–1279, https://doi.org/10.1007/s11666-018-0798-8.
[37] A. Lopera-Valle, A. McDonald, Flame-sprayed coatings as de-icing elements for fiber-reinforced polymer composite structures: modeling and experimentation, Int. J. Heat Mass Transf. 97 (2016) 56–65, https://doi.org/10.1016/j.ijheatmasstransfer.2016.01.079.
[38] V. Donadei, H. Koivuluoto, E. Sarlin, P. Vuoristo, Icephobic behaviour and thermal stability of flame-sprayed polyethylene coating: the effect of process parameters, J. Therm. Spray Technol. 29 (2019) 241–254, https://doi.org/10.1007/s11666-019-00947-0.
[39] J. Zhou, K. Sun, S. Huang, X. He, W. Cai, Y. Zhao, W. Li, Facile fabrication of polyimide-alumina composite coatings by liquid flame spray, Coatings 10 (2020), https://doi.org/10.3390/coatings10090857.
[40] Y. Liu, X. Suo, Z. Wang, Y. Gong, X. Wang, H. Li, Developing polyimide-copper antifouling coatings with capsule structures for sustainable release of copper, Mater. Des. 130 (2017) 285–293, https://doi.org/10.1016/j.matdes.2017.05.075.
[41] M. Bayrakci, M. Keskinates, B. Yilmaz, Antibacterial, thermal decomposition and in vitro time release studies of chloramphenicol from novel pla and pva nanofiber mats, Mater. Sci. Eng. C Mater. Biol. Appl. 122 (2021), 111895, https://doi.org/10.1016/j.msec.2021.111895.
[42] K. Polak-Krasna, A.R. Abaei, R.N. Shirazi, E. Parle, O. Carroll, W. Ronan, T. J. Vaughan, Physical and mechanical degradation behaviour of semi-crystalline plla for bioresorbable stent applications, J. Mech. Behav. Biomed. Mater. 118 (2021), 104409, https://doi.org/10.1016/j.jmbbm.2021.104409.
[43] J.E. Báez, Á. Marcos-Fernández, A comparison of three different biodegradable aliphatic oligoesters (pga, plla, and pcl) with similar linear alkyl end groups by dsc and saxs, Int. J. Polym. Anal. Charact. 20 (2015) 637–644, https://doi.org/10.1080/1023666x.2015.1054138.
[44] A. Rezzoug, S. Abdi, A. Kaci, M. Yandouzi, Thermal spray metallisation of carbon fibre reinforced polymer composites: effect of top surface modification on coating adhesion and mechanical properties, Surf. Coat. Technol. 333 (2018) 13–23, https://doi.org/10.1016/j.surfcoat.2017.10.066.
[45] M.S. Rihawy, A. Alzier, A.W. Allaf, Investigation of chloramphenicol release from pva/cmc/hea hydrogel using ion beam analysis, uv and ftir techniques, Appl. Radiat. Isot. 153 (2019), 108806, https://doi.org/10.1016/j.apradiso.2019.108806.
[46] T.T.T. Trang, M. Mariatti, H.Y. Badrul, K. Masakazu, X.T.T. Nguyen, A.A. H. Zuratul, Drug release profile study of gentamicin encapsulated poly(lactic acid) microspheres for drug delivery, Mater. Today: Proceedings 17 (2019) 836–845, https://doi.org/10.1016/j.matpr.2019.06.370.
[47] I.J. Macha, B. Ben-Nissan, E.N. Vilchevskaya, A.S. Morozova, B.E. Abali, W. H. Muller, W. Rickert, Drug delivery from polymer-based nanopharmaceuticals-an experimental study complemented by simulations of selected diffusion processes, Front. Bioeng. Biotechnol. 7 (2019) 37, https://doi.org/10.3389/fbioe.2019.00037.
[48] V. Kumari, P. Tyagi, A. Sangal, In-vitro kinetic release study of illicium verum (chakraphool) polymeric nanoparticles, Mater. Today: Proceedings 60 (2022) 14–20, https://doi.org/10.1016/j.matpr.2021.11.014.
[49] M.A. Abushaheen, A.J. Muzaheed, M. Fatani, W. Alosaimi, M. Mansy, S. George, S. Acharya, D.D. Rathod, C. Divakar, S. Jhugroo, A.A. Vellappally, J. Khan, Shaik, P. Jhugroo, Antimicrobial resistance, mechanisms and its clinical significance, Dis. Mon. 66 (2020), 100971, https://doi.org/10.1016/j.disamonth.2020.100971.
[50] F. Nazir, M. Iqbal, A.N. Khan, M. Mazhar, Z. Hussain, Fabrication of robust poly l-lactic acid/cyclic olefinic copolymer (plla/coc) blends: study of physical properties, structure, and cytocompatibility for bone tissue engineering, J. Mater. Res. Technol. 13 (2021) 1732–1751, https://doi.org/10.1016/j.jmrt.2021.05.073.
[51] Y. Srisuwan, Y. Baimark, Improvement of water resistance of thermoplastic starch foams by dip-coating with biodegradable polylactide-b-polyethylene glycol-b-polylactide copolymer and its blend with poly(d-lactide), Prog. Org. Coat. 151 (2021), https://doi.org/10.1016/j.porgcoat.2020.106074.
[52] E.M. Abdelrazek, A.M. Hezma, A. El-khodary, A.M. Elzayat, Spectroscopic studies and thermal properties of pcl/pmma biopolymer blend, Egypt. J. Basic Applied Sci. 3 (2019) 10–15, https://doi.org/10.1016/j.ejbas.2015.06.001.

[53] J. Meng, F. Boschetto, S. Yagi, E. Marin, T. Adachi, X. Chen, G. Pezzotti, S. Sakurai, S. Sasaki, T. Aoki, H. Yamane, H. Xu, Enhancing the bioactivity of melt electrowritten plla scaffold by convenient, green, and effective hydrophilic surface modification, Mater. Sci. Eng. C Mater. Biol. Appl. 135 (2022), 112686, https://doi.org/10.1016/j.msec.2022.112686.
[54] H. Peng, Y. Han, T. Liu, W.C. Tjiu, C. He, Morphology and thermal degradation behavior of highly exfoliated coal-layered double hydroxide/polycaprolactone nanocomposites prepared by simple solution intercalation, Thermochim. Acta 502 (2010) 1–7, https://doi.org/10.1016/j.tca.2010.01.009.
[55] K. Sownthari, S.A. Suthanthiraraj, Synthesis and characterization of an electrolyte system based on a biodegradable polymer, Express Polym Lett 7 (2013) 495–504, https://doi.org/10.3144/expresspolymlett.2013.46.
[56] X.W. Li, X.H. Lin, L.Q. Zheng, L. Yu, H.Z. Mao, Preparation, characterization, and in vitro release of chloramphenicol loaded solid lipid nanoparticles, J. Dispers. Sci. Technol. 29 (2010) 1214–1221, https://doi.org/10.1080/01932690701856782.
[57] J. Choi, B.N. Jang, B.J. Park, Y.K. Joung, D.K. Han, Effect of solvent on drug release and a spray-coated matrix of a sirolimus-eluting stent coated with poly(lactic-co-glycolic acid), Langmuir 30 (2014) 10098–10106, https://doi.org/10.1021/la500452h.
[58] F. Lu, Y.Y. Shen, Y.Q. Shen, J.W. Hou, Z.M. Wang, S.R. Guo, Treatments of paclitaxel with poly(vinyl pyrrolidone) to improve drug release from poly (varepsilon-caprolactone) matrix for film-based stent, Int. J. Pharm. 434 (2012) 161–168, https://doi.org/10.1016/j.ijpharm.2012.05.043.
[59] Y. Zhang, T. Shams, A.H. Harker, M. Parhizkar, M. Edirisinghe, Effect of copolymer composition on particle morphology and release behavior in vitro using progesterone, Mater. Des. 159 (2018) 57–67, https://doi.org/10.1016/j.matdes.2018.08.024.
[60] E. Sanchez-Rexach, E. Meaurio, J. Iturri, J.L. Toca-Herrera, S. Nir, M. Reches, J.-R. Sarasua, Miscibility, interactions and antimicrobial activity of poly (ε-caprolactone)/chloramphenicol blends, Eur. Polym. J. 102 (2018) 30–37, https://doi.org/10.1016/j.eurpolymj.2018.03.011.
[61] J. Urquijo, G. Guerrica-Echevarría, J.I. Eguiazábal, Melt processed pla/pcl blends: effect of processing method on phase structure, morphology, and mechanical properties, J. Appl. Polym. Sci. 132 (2015), https://doi.org/10.1002/app.42641.
[62] A. Chavez-Valdez, A. Arizmendi-Morquecho, K.J. Moreno, J.A. Roether, J. Kaschta, A.R. Boccaccini, Tio2–plla nanocomposite coatings and free-standing films by a combined electrophoretic deposition-dip coating process, Compos. Part B-Eng. 67 (2014) 256–261, https://doi.org/10.1016/j.compositesb.2014.07.001.
[63] C. Song, Y. Yang, Y. Zhou, L. Wang, S. Zhu, J. Wang, R. Zeng, Y. Zheng, S. Guan, Electrochemical polymerization of dopamine with/without subsequent plla coating on mg-zn-y-nd alloy, Mater. Lett. 252 (2019) 202–206, https://doi.org/10.1016/j.matlet.2019.04.122.
[64] J. Hu, J. Wang, M. Wang, Y. Ozaki, H. Sato, J. Zhang, Investigation of crystallization behavior of asymmetric plla/pdla blend using raman imaging measurement, Polymer 172 (2019) 1–6, https://doi.org/10.1016/j.polymer.2019.03.049.
[65] J. Guan, W. Luo, S. Lu, Y. Yang, X. Shen, B. Tang, Y. Li, Synchronous toughening and strengthening of the immiscible polylactic acid/thermoplastic polyurethane (plla/tpu) blends via the interfacial compatibilization with janus nanosheets, Compos. Sci. Technol. 227 (2022), https://doi.org/10.1016/j.compscitech.2022.109611.
[66] Y. Zhang, D. Wu, M. Zhang, W. Zhou, C. Xu, Effect of steady shear on the morphology of biodegradable poly(ε-caprolactone)/polylactide blend, Polym. Eng. Sci. 49 (2009) 2293–2300, https://doi.org/10.1002/pen.21456.
[67] I. Navarro-Baena, V. Sessini, F. Dominici, L. Torre, J.M. Kenny, L. Peponi, Design of biodegradable blends based on pla and pcl: from morphological, thermal and mechanical studies to shape memory behavior, Polym. Degrad. Stab. 132 (2016) 97–108, https://doi.org/10.1016/j.polymdegradstab. 2016.03.037.
[68] Z. Qi, H. Yu, Y. Chen, M. Zhu, Highly porous fibers prepared by electrospinning a ternary system of nonsolvent/solvent/poly(l-lactic acid), Mater. Lett. 63 (2009) 415–418, https://doi.org/10.1016/j.matlet.2008.10.059.
[69] Q. Yang, L. Chen, X. Shen, Z. Tan, Preparation of polycaprolactone tissue engineering scaffolds by improved solvent casting/particulate leaching method, J. Macromol. Sci. B 45 (2006) 1171–1181, https://doi.org/10.1080/00222340600976783.
[70] T. Hongthipwaree, P. Sriamornsak, M. Seadan, S. Suttiruengwong, Effect of cosolvent on properties of non-woven porous neomycin-loaded poly(lactic acid)/polycaprolactone fibers, Mate. Today Sustain. 10 (2020), https://doi.org/10.1016/j.mtsust.2020.100051.
[71] J. Rogalski, C. Bastiaansen, T. Peijs, Pa6 nanofibre production: a comparison between rotary jet spinning and electrospinning, Fibers 6 (2018), https://doi.org/10.3390/fib6020037.
[72] H. Wang, W. Li, Z. Li, Preparation of fluorinated pcl porous microspheres and a super-hydrophobic coating on fabrics via electrospraying, Nanoscale 10 (2018) 18857–18868, https://doi.org/10.1039/c8nr05793a.
[73] Y. Du, X. Chen, Y. Hag Koh, B. Lei, Facilely fabricating pcl nanofibrous scaffolds with hierarchical pore structure for tissue engineering, Mater. Lett. 122 (2014) 62–65, https://doi.org/10.1016/j.matlet.2014.02.031.
[74] H.H. Tuson, D.B. Weibel, Bacteria-surface interactions, Soft Matter 9 (2013) 4368–4380, https://doi.org/10.1039/C3SM27705D.
[75] K. Szustakiewicz, M. Gazińska, B. Kryszak, M. Grzymajło, J. Pigłowski, R. J. Wiglusz, M. Okamoto, The influence of hydroxyapatite content on properties of poly(l-lactide)/hydroxyapatite porous scaffolds obtained using thermal induced phase separation technique, Eur. Polym. J. 113 (2019) 313–320, https://doi.org/10.1016/j.eurpolymj.2019.01.073.
[76] X.H. Wu, Z.Y. Wu, J.C. Su, Y.G. Yan, B.Q. Yu, J. Wei, L.M. Zhao, Nano-hydroxyapatite promotes self-assembly of honeycomb pores in poly(l-lactide) films through breath-figure method and mc3t3-e1 cell functions, RSC Adv. 5 (2015) 6607–6616, https://doi.org/10.1039/c4ra13843k.
[77] B.K.D. Ngo, M.A. Grunlan, Protein resistant polymeric biomaterials, ACS Macro Lett. 6 (2017) 992–1000, https://doi.org/10.1021/acsmacrolett.7b00448.
[78] Y.S. Lui, M.P. Lewis, S.C. Loo, Sustained-release of naproxen sodium from electrospun-aligned plla-pcl scaffolds, J. Tissue Eng. Regen. Med. 11 (2017) 1011–1021, https://doi.org/10.1002/term.2000.
[79] S. Liu, J. Yu, H. Li, K. Wang, G. Wu, B. Wang, M. Liu, Y. Zhang, P. Wang, J. Zhang, J. Wu, Y. Jing, F. Li, M. Zhang, Controllable drug release behavior of polylactic acid (pla) surgical suture coating with ciprofloxacin (cpfx)-polycaprolactone (pcl)/polyglycolide (pga), Polymers (Basel) 12 (2020), https://doi.org/10.3390/polym12020288.
[80] A.G. Cid, F. Sonvico, R. Bettini, P. Colombo, E. Gonzo, A.F. Jimenez-Kairuz, J. M. Bermudez, Evaluation of the drug release kinetics in assembled modular systems based on the dome matrix technology, J. Pharm. Sci. 109 (2020) 2819–2826, https://doi.org/10.1016/j.xphs.2020.06.006.